Spatially congruent negative BOLD responses to different stimuli do not summate in visual cortex

Wilson, Ross; Thomas, Andrea; Mayhew, Stephen

DOI:
10.1016/j.neuroimage.2020.116891

Document Version
Publisher's PDF, also known as Version of record

Citation for published version (Harvard):
Wilson, R, Thomas, A & Mayhew, S 2020, 'Spatially congruent negative BOLD responses to different stimuli do not summate in visual cortex', *NeuroImage*, vol. 218, 116891. https://doi.org/10.1016/j.neuroimage.2020.116891

NeuroImage 218 (2020) 116891

Contents lists available at ScienceDirect

NeuroImage

journal homepage: www.elsevier.com/locate/neuroimage

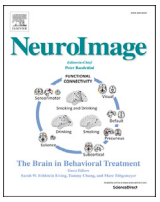

Spatially congruent negative BOLD responses to different stimuli do not summate in visual cortex

Ross Wilson, Andrea Thomas, Stephen D. Mayhew *

Centre for Human Brain Health (CHBH), School of Psychology, University of Birmingham, Birmingham, UK

A B S T R A C T

The negative BOLD response (NBR) is a prevalent feature of brain activity during sensory and cognitive tasks. It is thought to reflect suppression or deactivation of cortical areas unrequired for task performance, but much remains to be understood regarding its response properties and generative pathways. Here we study a unique property of sensory cortex NBR that most distinguishes it from positive BOLD responses (PBR), its appearance in a single location due to different stimuli. We investigate whether such NBR are additive, as a means of studying whether stimulus driven NBR arise via a single or multiple pathways.

During fMRI, subject's passively viewed separate checkerboard stimulation of the foveal and middle-eccentricity areas of the left visual field and a third condition that stimulated both areas concurrently. PBR was observed in the contralateral primary visual cortex and NBR was seen throughout the ipsilateral cortex as well as in contralateral regions superior and anterior to the PBR. Strong spatial overlap of NBRs to all three conditions was observed.

We found that neither PBR nor NBR were additive. NBR amplitudes to combined stimuli were equal to those of the strongest (foveal) stimulus alone, despite the mid-eccentricity stimulus inducing substantial NBR on its own. The lack of summation of NBRs, both in the same and opposite hemispheres to the PBR, suggests that they arise from a single pathway. Our findings suggest that although individual stimuli each exert a separate inhibitory effect on non-stimulated regions, once in combination these effects operate as a binary system. Deactivation of a given visual area is driven by a single signal, representing only the largest of the contributing sources.

1. Introduction

Blood oxygenation-level dependent (BOLD) functional magnetic resonance imaging (fMRI) is a widely used neuroimaging technique (Kwong et al., 1992; Ogawa et al., 1990) for indirectly inferring the spatial location and magnitude of brain function via the haemodynamic correlates of neural activity (Heeger et al., 2000; Logothetis, 2002). The most commonly analysed measure is an increase in BOLD signal above baseline (or "resting") levels. This is known as a positive BOLD response (PBR) and taken as a measure of increased local field potential activity and synaptic input resulting from the presentation of a stimulus (Logothetis et al., 2001; Viswanathan and Freeman, 2007). Another prominent BOLD signal is the negative BOLD response (NBR), a decrease in signal below baseline following stimulation. NBR are commonly observed but much less widely studied and applied in neuroimaging due to lingering uncertainties concerning their precise interpretation.

The NBR manifests in a variety of ways: within (intra modal) and between (cross modal) sensory modalities as well as in the default mode network (DMN) (Raichle et al., 2001; Raichle and Snyder, 2007). Intra modal NBR are widely observed in visual or sensorimotor cortex representations of unstimulated portions of the sensory field (Hlushchuk and Hari, 2006; Kastrup et al., 2008; Mayhew et al., 2013b; Newton et al., 2005; Shmuel et al., 2002; Smith et al., 2000, 2004), whereas cross modal NBR are reported in sensory cortices not recruited by the stimulation paradigm (Hairston et al., 2008; Mayhew et al., 2013a, 2013b; Mozolic et al., 2008; Wilson et al., 2019) e.g. deactivation of auditory cortex during a visual task.

NBR are of interest as they offer the potential for neuroimaging research to move beyond primarily studying activations to measuring another aspect of brain activity, that of functional inhibition or down-regulation of regions unnecessary for task performance. Initially, it was suggested that NBR arose from vascular mechanisms (Devor et al., 2005; Harel et al., 2002; Kannurpatti and Biswal, 2004), reflecting passive changes in blood flow/volume unrelated to neuronal activity. Whilst this theory remains relevant in specific cases (Bianciardi et al., 2011; Puckett et al., 2014) an emerging consensus suggests that a substantial component of cortical NBR has neuro-metabolic origins (Mullinger et al., 2014; Pasley et al., 2007; Schafer et al., 2012; Shmuel et al., 2002; Sten et al., 2017) associated with decreased gamma-frequency LFP activity in visual NBR in primates (Shmuel et al., 2006), sensorimotor NBR in rats (Boorman et al., 2010, 2015) and in DMN regions of human epilepsy patients (Jerbi et al., 2010). Whilst such studies suggests that NBR reflects, at least

* Corresponding author.
E-mail address: s.d.mayhew@bham.ac.uk (S.D. Mayhew).

https://doi.org/10.1016/j.neuroimage.2020.116891
Received 11 October 2019; Received in revised form 23 April 2020; Accepted 28 April 2020
Available online 11 May 2020

in part, a measure of cortical deactivation, it does not appear that NBR simply reflects the opposite of PBR (Huber et al., 2014; Mullinger et al., 2014). Currently, many aspects of knowledge about NBR remain incomplete such as its: generative signalling pathways, underlying ratio of changes of excitatory and inhibitory activity, neurovascular coupling, and relationship to task activation (PBR).

Intra modal visual NBR are the most widely studied sensory NBR. It has been shown Visual NBR contains information that discriminates different Gabor stimulus patterns (Bressler et al., 2007) and its amplitude is modulated by stimulus intensity and duration in a manner comparable to that of the PBR (Shmuel et al., 2002). Often bilateral rings of high contrast checkers are displayed to the fovea and periphery of visual field which induce bilateral NBR in peripheral and foveal visual cortex respectively in an eccentricity dependent manner (Pasley et al., 2007; Shmuel et al., 2002, 2006; Wade and Rowland, 2010). Other studies using unilateral stimuli observed NBR throughout the ipsilateral visual cortex (Fracasso et al., 2018; Gouws et al., 2014; Mayhew et al., 2013b; Smith et al., 2004; Wilson et al., 2019).

This spatial extent is a property that most distinguishes NBR from PBR. Whereas PBR occurs in a retinotopic pattern, specifically localising the activated neural population, NBR is observed across all visual cortex representations of unstimulated areas of the visual field. Therefore, visual NBR can occur either surrounding the PBR within the stimulated hemisphere (Pasley et al., 2007; Shmuel et al., 2002), or in the hemisphere opposite to the activation (Mayhew et al., 2013b; Smith et al., 2004; Wilson et al., 2019). This property means that a variety of stimulus shapes and categories could give rise to NBR in a given visual region, potentially leading to an ambiguous link between the stimulus and NBR.

This presents the opportunity for the present study to improve understanding of fundamental response properties of NBR by investigating how NBRs spatial distribution between visual hemispheres varies with stimulus location and how NBR amplitudes are affected by combining stimuli that each separately induce NBR in specific cortical locations. In doing so, we also take the opportunity to investigate the potential signalling pathways by which NBR arises.

We studied NBR induced in the visual cortex by passive observation of small visual checkerboard stimuli. In two separate conditions different portions of the left hemifield (fovea (F) and middle (M) eccentricity) were stimulated and then a third condition stimulated both concurrently (FM). We aimed to induce NBR in the whole of the ipsilateral visual cortex as well as the peripheral representation of the contralateral cortex. We compared the NBR magnitude and spatial extent between the three conditions in order to determine whether stimulation of two distinct portions (F and M) of the visual field created similar extent of NBR, with overlap in the contralateral and/or ipsilateral hemisphere; or alternatively were the two NBRs retinotopically specific to each stimulus?

Based on the indications of previous work (Mayhew et al., 2013b; Shmuel et al., 2002; Smith et al., 2004; Wandell et al., 2007) we hypothesize that stimulation of spatially distinct portions of the visual field will create retinotopically specific activations (PBRs) in visual cortex but will induce spatially overlapping NBR across all unstimulated parts of visual cortex that are similarly not required for processing the stimuli. We expect the strongest magnitude NBR to all conditions to be observed in posterior ipsilateral V1 (Gouws et al., 2014; Mayhew et al., 2013b), the foveal representation of the right hemifield, opposite the area of strongest PBR in contralateral V1.

Therefore, when two portions of the visual field are stimulated concurrently (FM stimuli) we further investigate the additivity of NBR, specifically whether:

1. The NBR to FM is greater-than, equal-to, or lesser-than the sum of the NBRs to F and M stimuli alone. Or phrased another way: are bottom-up, stimulus-driven NBR additive?
2. The NBR additivity is consistent across all visual areas, or different between contralateral and ipsilateral NBR.

Investigating if NBRs are additive is the primary goal of this paper, but this leads to consideration of a secondary and interlinked issue of what signals may initiate the NBR and whether NBR amplitude reflects the integration of separate stimulus inputs that each drive a response in that location. The bulk of current evidence suggests that cortical NBR arises from a net reduction in excitation and local metabolic demand (Boorman et al., 2015; Lauritzen et al., 2012; Mullinger et al., 2014; Schafer et al., 2012; Shmuel et al., 2002, 2006) which could arise from: a reduction in afferent excitatory input from another region; and/or a local increase in the activity of inhibitory neurons acting to suppress neighbouring excitatory neurons. We suggest three primary mechanisms that could contribute to the suppression of excitatory activity underlying NBR: 1) thalamocortical interaction, such as when closing the eyes induces NBR in visual cortex (Feige et al., 2005) or lateral geniculate nucleus (LGN) stimulation inducing visual NBR outside of the retinotopically stimulated region (Logothetis et al., 2010); 2) intra-cortical connectivity such as that suggested between sensorimotor hemispheres (Ferbert et al., 1992; Kastrup et al., 2008; Klingner et al., 2010; Schafer et al., 2012) or different sensory cortices (Iurilli et al., 2012); and top-down control of attention (Heinemann et al., 2009; Tootell et al., 1998) by fronto-parietal circuits (Lauritzen et al., 2009).

In the current study we used passive stimuli to primarily induce visual NBR via stimulus driven, bottom up generative mechanisms and minimise the potential contribution of top-down spatial attention (Bressler et al., 2013). We attempt to elucidate whether these NBR arise via a single pathway or from multiple pathways. If both F and M stimuli lead to transmission of separate inhibitory signals acting on one location, then the NBR induced by FM stimuli would be expected to reflect the sum of the two, resulting in an NBR that increases with the level of input. Such a mechanism would most likely reflect a feedforward thalamic pathway whereby each separate input makes a contribution to the NBR generation. If however a single signalling pathway is responsible for regional deactivation, then it may behave as a more binary system, whereby only the largest of the two inhibitory signals is transmitted e.g. the NBR to FM stimuli is not larger than NBR to F alone. Such a mechanism would be consistent with an intra-cortical pathway whereby cortical integration of stimulus inputs results in a single inhibitory signal initiating visual NBR. We study these effects across both visual hemispheres as contralateral NBR (within the same hemisphere as the PBR) could rely on local, lateral inhibition effects between neighbouring cortical regions and may not arise from the same mechanism as ipsilateral NBR which could depend on inter-hemispheric communication.

2. Materials and methods

3T BOLD fMRI data were recorded at the Birmingham University Imaging Centre (BUIC). Sixteen young adult subjects (age 21 ± 4 yrs (mean ± s.d.), 6 female) were recruited by opportunity sampling from the undergraduate student population. All subjects had normal or corrected to normal vision as established by reading a standardised letter eye-chart. This study was conducted with the approval of the University of Birmingham local ethics committee and all subjects provided informed consent.

2.1. Paradigm

Visual stimuli were projected onto a screen at the rear of the scanner bore and viewed via a mirror mounted on the scanner's head coil. Subjects were instructed to fixate throughout on a centrally displayed red dot displayed on a grey background. Subjects were instructed to passively view three conditions of left-hemifield radial, black-white checkerboard stimuli. Stimuli were shown at 100% contrast, reversing contrast at 7.5Hz. The grey background was isoluminant with all stimuli. Two of the conditions featured checkerboards at different locations in the visual field (Fig. 1). The locations of the stimuli were: left foveal (F, 0.5–2.5°); upper left mid-eccentricity (M, 5.5–7°). The third condition was the

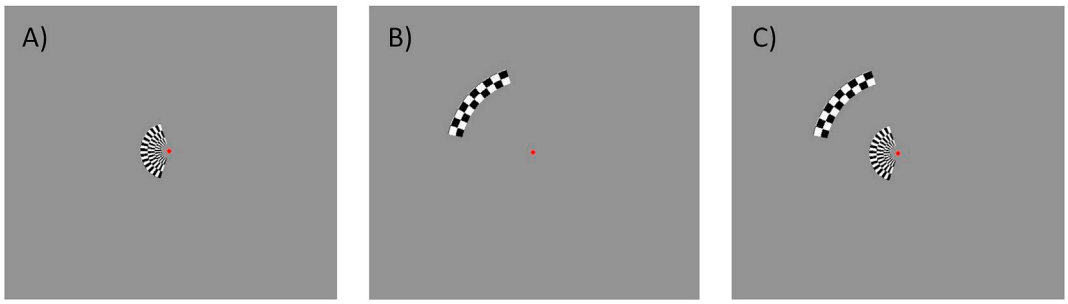

Fig. 1. Visual display of the checkerboard stimuli that comprised the three experimental conditions: A) left foveal (F); B) upper left mid-eccentricity (M); C) both left foveal and upper left mid-eccentricity (FM).

combination of both these two stimuli (FM), presented concurrently. The stimuli were designed such that all three conditions induced NBR in peripheral regions of contralateral visual cortex as well as throughout ipsilateral visual cortex. Our analysis would investigate whether the NBR to the FM condition was greater than, less than, or equal to the NBR combined from the separate F and M conditions.

Each subject completed three experimental runs of the task. Each run consisted of a 10s initial baseline period of resting fixation followed by 18 trials, 6 trials of each stimulus condition, presented in a pseudo-randomised order. All stimuli (F, M or FM) were delivered for 10 s, separated by resting fixation intervals of either 16 or 17 s, counter-balanced across conditions, and designed to provide good sampling of the haemodynamic response across 2s TR periods.

A total of 18 trials per condition were recorded. Subjects also completed an additional 10-min, localiser experiment, where 6s duration checkerboard stimuli alternated presentation between 10 locations in the visual field: the left and right fovea (0.5–3°) and the left and right regions of the upper and lower visual field at middle (4–8°) and peripheral (9–13°) eccentricities (see Figure S1). Activations to this localiser task were used to define regions of interest (ROIs) and allow interrogation of the spatial variation of NBR amplitude between conditions.

2.2. Data acquisition

MR data were recorded with a Philips Achieva 3T MR scanner (Philips Medical Systems, Best, Netherlands), with a body transmit coil and 32-channel receive head coil. The scanner's physiological monitoring system was used to record cardiac and respiratory cycles (PPU and respiratory belt). Gradient echo EPI was used to acquire T2*-weighted BOLD data with the following parameters: Multiband factor = 2, SENSE factor 2.3, TR = 2000 ms, TE = 38 ms, 2x2x2 mm^3 voxels, flip angle = 80°, FOV 144x144, 42 slices, 245 vol per run giving a run length of 8 min and 10 s. A whole-head T_1-weighted MPRAGE anatomical image with (TR = 2000 ms, TE = 2 ms, TI = 880 ms, flip angle = 8°, FOV 256x256, 1 mm isotropic resolution) was acquired to facilitate image co-registration.

2.3. Analysis

All BOLD data were preprocessed using FSL (www.fsl.fmrib.ox.ac.uk) including motion correction (MCFLIRT), spatial smoothing (4 mm Gaussian kernel) and registration to MNI space (FLIRT (Jenkinson et al., 2002),). The PPU and respiratory data of each subject were input to the PhysIO toolbox (Kasper et al., 2017), which was used to calculate time-course regressors that modelled variability in physiological noise. A total of 3 cardiac and 4 respiratory terms were used along with 1 interaction term, to create RETROICOR style regressors (Glover et al., 2000). In addition, the respiration per volume time (RVT) (Birn et al., 2008) and heart-rate variability (Chang et al., 2009) regressors were also modelled. These regressors were included in the first-level general linear model (GLM) design matrix, along with the six main parameters of head motion, as covariates of no interest.

Regressors modelling the BOLD response to each of the three conditions (F, M, FM) were constructed from the stimulus timings and convolved with a double gamma haemodynamic response function. Their temporal derivatives were also included in the design matrix. Both positive and negative contrasts were set at the first level, along with contrasts comparing responses between conditions (e.g. F vs FM and F + M > FM).

GLM analysis was performed with FEAT 6.0. Second level fixed-effects analysis across all runs was used to generate a mean response to each condition per subject. Third level fixed effects analysis then calculated group level results ($Z > 3.0$ $p < 0.05$ cluster corrected).

Localiser data were analysed using first-level GLMs that modelled separate events for all ten stimulus locations: left fovea, right fovea, left upper field periphery, right upper field periphery, left upper field middle, right upper field middle, left lower field middle, right lower field middle, left lower field periphery, right lower field periphery. Second and third level fixed effects analysis calculated group level PBR activations for each location ($Z > 3.0$ $p < 0.05$ cluster corrected). Ten group-level ROIs were then defined from the cluster with the most significant response in each of the group maps. These group ROIs were then registered to each subject's localiser data and used to locate the subject's peak response voxel for each localiser condition from their first-level GLM results. Subject-specific ROIs were defined by centering a 5 × 5 × 5 voxel cube on the peak voxel PBR to each stimulus location. For each of the F, M and FM conditions, we calculated the proportion of positively and negatively responding voxels in the ROI and used only the voxels with the dominant response, to avoid averaging together PBR and NBR. Mean BOLD time-courses were then extracted and the % BOLD signal change induced by F, M and FM conditions was calculated with respect to resting fixation baseline. The timecourse data were then averaged across runs and compared between conditions.

3. Results

Examination of motion parameters confirmed that no run had exceeded 4 mm absolute motion, so no data was excluded from analysis.

Fig. 2 displays group-level statistical maps of significant activation and deactivation to each of the visual stimulus conditions. It is important to understand how the PBR was affected by stimulus condition before interpreting the NBR.

3.1. Positive BOLD responses

F stimulation induced strongest PBR in posterior regions of the contralateral calcarine (cV1). This PBR encompassed both the upper and lower banks of the calcarine, as the foveal checkerboard was presented to both upper and lower quadrants of the left visual field. F stimuli also evoked PBR in bilateral inferior occipital cortex. In comparison, M stimulation induced strongest PBR in a central region of the lower part of cV1 (as the M checker was only present in the upper left visual field) as well as in contralateral inferior occipital cortex. During FM stimulation

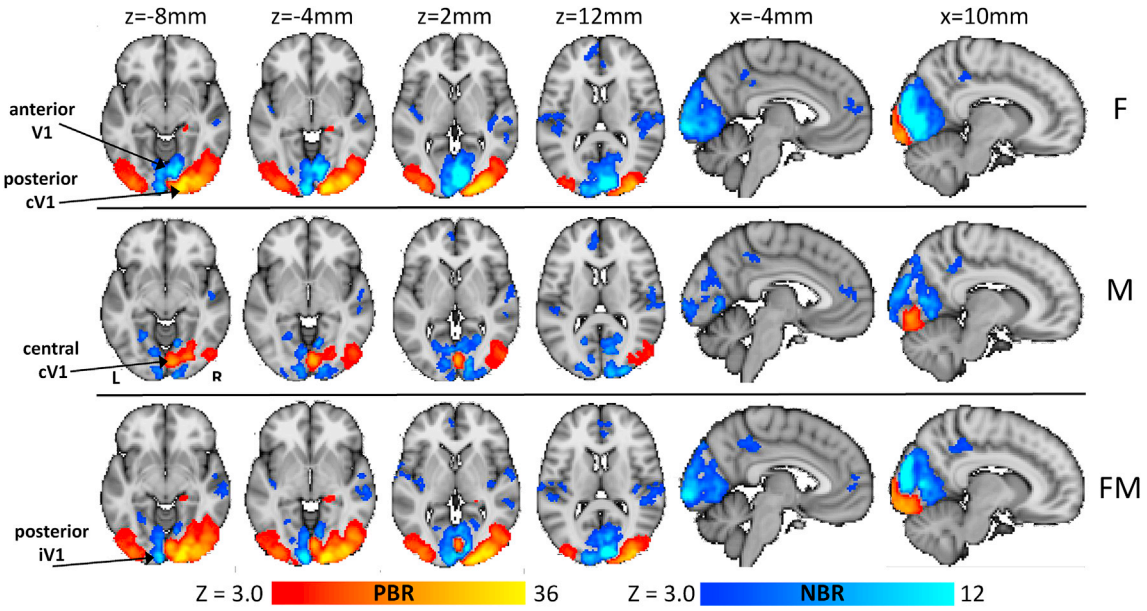

Fig. 2. Group mean GLM statistical maps showing regions of PBR (red/yellow) and NBR (blue) to each of the three conditions: F (top row), M (middle row) and FM (bottom row) stimulation. Sagittal images at −4 and 10 mm show ipsilateral and contralateral V1 respectively. All images fixed effects, cluster corrected $Z > 3$ and $p < 0.05$.

Table 1
Z-statistics and MNI co-ordinates of peak voxel PBR and NBR for each condition, for the most prominent contralateral (right) and ipsilateral (left) clusters as well as in auditory and DMN areas of NBR.

	F	M	FM
cV1 PBR – Peak Z-statistic	34.8	25.3	35.6
cV1 PBR – Peak co-ordinate	18,-96,-6	4,-82,-2	16,-98,-4
cV1 NBR – Peak Z-statistic	17.4	6.9	14.6
cV1 NBR – Peak co-ordinate	10,-88,4	14,-86,4	6,-92,8
iV1 NBR – Peak Z-statistic	10.4	5.3	11.3
iV1 NBR – Peak co-ordinate	−6,-98,-4	−8,-94,-4	−6,-98-4
Auditory Cortex NBR – Peak Z-statistic	5.9	3.9	4.6
Auditory Cortex NBR – Peak co-ordinate	52,-16,12	56,-24,10	60,-24,14
PCC NBR – Peak Z-statistic	3.8	3.7	5.3
PCC NBR – Peak co-ordinate	−2,-26,38	12,-44,36	2,-40,44

PBR was observed in all of these locations (see Table 1), as expected. The magnitude and extent of PBR to M stimulation was weaker than to either F or FM conditions. The PBR amplitude was highly comparable between F and FM conditions, with GLM contrast F vs FM showing no significant difference in posterior cV1. The only difference in PBR between F and FM (see Figure S2) was seen in the central contralateral calcarine region specifically stimulated by the M stimulus. This suggests that in general the FM PBR was the sum of the F and the M PBRs, with no additional regions or larger amplitudes seen in FM than in F + M. PBR was also observed in the contralateral lateral geniculate nucleus during the F and FM conditions, but this did not reach significance in the M condition. PBR was also observed in the ipsilateral hemisphere, but only in very lateral secondary visual regions beyond the calcarine which are not reported further.

3.2. Negative BOLD responses

Substantial NBR was evoked by each stimulus, see Fig. 2. NBR was seen in all areas of the visual cortex that were not directly stimulated by the checkerboards, as previously reported (Bressler et al., 2007; Pasley et al., 2007; Shmuel et al., 2002; Smith et al., 2004; Wade and Rowland, 2010), though most previous work used whole-field ring stimulation and did not specifically study ipsilateral NBR.

We observed that the magnitude, spatial extent and location of the NBR varied between the three conditions. For example, the F checkerboard (in the fovea of the left visual field) stimulated only the posterior contralateral calcarine cortex and therefore induced NBR throughout the ipsilateral (i) calcarine as well as anterior cV1 (the representation of the visual field periphery). This NBR was strongest in posterior iV1 (the visual cortex representation of the unstimulated right fovea) that was directly opposite the cV1 PBR see Fig. 2 and Table 1, and in a region of superior contralateral visual cortex, directly above the cV1 PBR.

The M condition induced NBR in bilateral calcarine cortex that surrounded the spot of PBR in central cV1. NBR was therefore observed both in the posterior cV1 and iV1 locations where the peak PBR and NBR to the F stimuli occurred respectively, as well bilateral anterior V1 regions where NBR was also seen to the F stimulus. This indicated that the mid eccentricity M stimulus could induce NBR in both foveal and peripheral visual representations. The considerable spatial overlap between F and M NBR is shown explicitly in Fig. 3. It is particularly within these areas that were interested to see how the FM NBR magnitude compared to that of F and M separately. The magnitude of the NBR to the M stimulus was weaker than that seen to the F stimulus, as shown by a GLM contrast between F and M, which showed that NBR was significantly larger during F than M stimuli in iV1 and superior visual cortex (Figure S3).

The spatial pattern of NBR to the FM stimulus closely resembled the combination of F and M, as expected. The FM NBR was seen in the same ipsilateral V1, anterior cV1 and dorsal visual regions that showed NBR to the F stimuli. FM NBR occurred in a ring around the central PBR region, the area of peak PBR to M. This included the region between the peak F and peak M PBR, in the visual cortex representation of the space between the foveal and mid-eccentric rings, showing that our stimuli evoked spatially distinct responses. Overall, as expected, a smaller spatial extent of NBR was seen to FM than to F stimuli, due to the extra activation caused by the additional M stimulus.

A significant difference in NBR magnitude was found between F and M conditions in posterior iV1 and anterior cV1. No difference in NBR was seen between F and FM conditions in any area, suggesting that the extra M stimulus did not result in enhancing the total NBR, despite both F and M stimuli separately inducing NBR in overlapping regions. To further illustrate this point Fig. 4 shows regions where the NBR magnitude to FM was significantly smaller than the sum of the separate NBR to F and M. Or put another way, the purple regions in Fig. 4 show that the NBR in visual cortex was not additive, as the NBR to FM was less than what would be

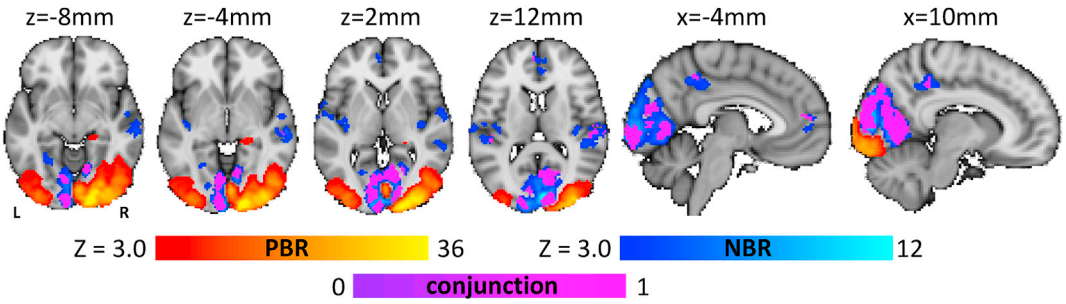

Fig. 3. Spatial conjunction (purple) of F NBR and M NBR superimposed on the PBR (red/yellow) and NBR (blue) to FM stimulation (same as shown in Fig. 1). Therefore purple areas show that overlapping NBR to both F and M stimuli were observed across widespread visual regions both ipsilateral and contralateral to the stimulation.

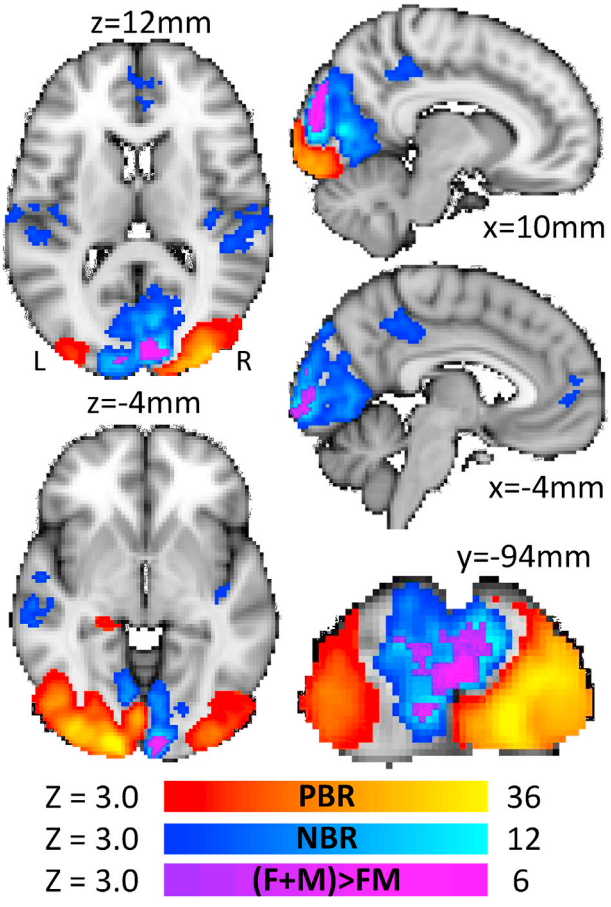

Fig. 4. GLM statistical map showing group contrast of (F + M)>FM (purple) superimposed on the PBR (red/yellow) and NBR (blue) to FM stimulation. All images fixed effects, cluster corrected $Z > 3$ and $p < 0.05$. Purple areas therefore denote regions where the NBR to FM was sub-additive, i.e. NBR to FM was of smaller magnitude than to F + M.

expected from the summation of overlapping F and M NBRs.

In addition, all three conditions induced a cross-modal NBR in bilateral auditory cortex (Hairston et al., 2008; Mozolic et al., 2008) and also NBR in small regions of the posterior cingulate cortex (PCC) and medial prefrontal cortex, reflecting deactivation of the default mode network (DMN) (McKiernan et al., 2003; Raichle et al., 2001). No difference in the amplitudes of auditory or DMN NBR was observed between conditions. Although curiously we note that the spatial pattern of these NBR appears to differ, as the conjunction of F and M NBR is small compared to the extent of the FM response in both auditory and PCC regions.

4. Region of interest analysis

The final analysis further evaluated and compared the magnitude of the NBRs between each condition for different regions of visual cortex. Fig. 5 plots the group mean BOLD response for each condition, arranged corresponding to the ten visual field locations used to extract the responses (see legend). Of most interest are Fig. 5B, E, F and H.

Fig. 5F shows the group mean BOLD responses from contralateral posterior V1, the region containing the peak PBR to the foveal stimuli in both the F and the FM conditions. The PBR to F (2.42% ± 0.31) and FM (2.52% ± 0.30) stimuli displayed very similar amplitudes in cV1 (students t-test, non-significant difference, $p = 0.89$) and additionally showed a large NBR during M (−0.65% ± 0.10) stimuli. Measures are group mean ± standard error in the mean.

In comparison, Fig. 5H shows the mid-eccentricity region of the lower calcarine which contained the peak PBR to the M stimuli. Consequently both M (1.93% ± 0.32) and FM (2.10% ± 0.28) stimuli showed a strong PBR with very similar amplitudes ($p = 0.78$), whilst an NBR was seen during F (−0.81% ± 0.12) stimuli. These results further evidence how visual cortex regions are deactivated if they do not represent the portion of visual field being stimulated.

The remaining panels of Fig. 5 plot responses from visual regions that displayed NBR during all three conditions. Fig. 5B&E shows responses from the two strongest areas of NBR, superior cV1 and posterior iV1 respectively. In superior cV1 the group mean NBR amplitude was: F (−0.9% ± 0.15); M (−0.32% ± 0.07); FM (−0.85% ± 0.15). Whereas in iV1 the group mean NBR amplitude was: F (−0.92% ± 0.08); M (−0.66% ± 0.1); FM (−0.97% ± 0.09).

In both these regions we found no difference between the NBR magnitudes for F and FM stimuli (superior cV1 $p = 0.81$; and posterior iV1 $p = 0.69$), despite a substantial NBR being observed separately to the M stimuli. In superior cV1, the NBR to M stimuli was 36% of the amplitude of NBR to F stimuli. If F and M NBRs were linearly additive in this region we would expect an FM NBR signal change of at least −1.2%, whereas we observe −0.85%. In iV1 the NBR to M stimuli was twice as strong as in superior cV1, at 71% of the NBR seen during F stimuli. If F and M NBRs were linearly additive in iV1 we would expect an FM NBR of at least −1.5%, whereas we observe −0.97%. Therefore we conclude that the NBRs elicited by separate passive visual stimuli are not additive and that NBR appears to approximate the amplitude of the largest contribution.

Broadly similar patterns were observed in the remaining regions, though the overall amplitudes of the NBR are smaller than in Fig. 5E&F, there is no difference between F and FM responses and the NBR to M is smaller than F or FM, but still clearly present. Finally, we observe no differences in the latency or the shape of the responses between conditions, in any of the ROIs.

5. Discussion

This BOLD fMRI study investigated the contribution to visual cortex

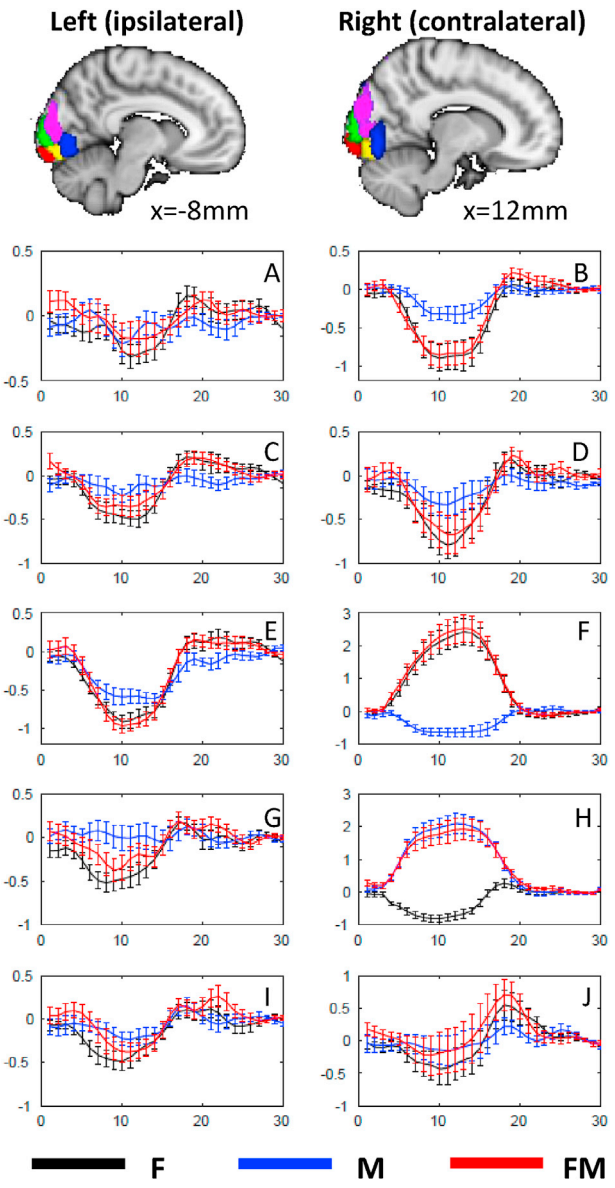

Fig. 5. Group mean BOLD responses to F (black), M (blue) and FM (red) stimuli extracted from ten different locations in visual cortex. Subject specific ROIs were defined during separate eccentricity mapping but to provide a summary the group-level ROIs are shown on the top row of brain images. Error bars denote ± standard error in the mean. The left column shows data from the ipsilateral (left) and the right column shows data from the contralateral (right) hemisphere. The central row of timecourses (E,F) are measured from posterior V1 (red ROI), the occipital pole, representing the visual field fovea. Upper panels (C,D) and (A,B) show middle and peripheral regions (green, purple ROIs)) of the upper bank of the calcarine respectively, that respond to stimuli of increasing eccentricity in the lower visual field. Lower panels (G–H) and (I–J) show middle and peripheral regions (yellow, blue ROIs)) of the lower bank of the calcarine (that respond to upper visual field stimuli). Panel F contains the peak PBR to F and FM stimuli. Panel H contains the peak PBR to M stimuli. Panel E contains the peak NBR to all stimuli.

NBR magnitude made by visual stimuli presented in two distinct locations (foveal F, mid-eccentricity M) of the visual field. NBR, measured relative to resting fixation baseline, that were evoked by each stimulus individually were compared to the NBR to the stimuli shown concurrently. We aimed to improve understanding of interactions between independent NBR sources and the generative processes underlying NBR. We hypothesized that if the two separate stimuli both triggered separate suppressive signalling pathways that induce reductions of BOLD signal in other visual regions, then when presented together these two stimulus effects would summate and result in stronger magnitude NBR.

Our results suggest that NBRs do not occur independently from each other, in the manner that PBRs are observed. Combining our F and M stimuli resulted in a greater area of total stimulated visual field thereby increasing the total stimulus input. We observed that the spatial extent of the PBR increased as the area of stimulated visual field increased (greater to FM compared with F or M). However, because of the different retinotopic representations of the F and M stimuli (shown by spatially distinct peak locations of PBR to F and M; and by similar PBR amplitudes for F and FM in posterior cV1) it was theorised this would lead to separate initiations of NBR. Although the F and M stimuli both induced NBR across overlapping regions of visual cortex, when combined in the FM condition these NBR were not independent of each other. Neither the PBR or NBR to the FM stimulus were additive in any region studied, meaning that their magnitudes were not different from the response to the F stimulus alone. This suggests that the strongest NBR generating signal (foveal, F) dominated in these conditions and no extra contribution to NBR was made from the other (M) stimulus.

5.1. *Spatial overlap of NBR and regional variation of NBR in visual cortex*

We observed widespread NBR across both hemispheres of the visual cortex during unilateral, left hemifield stimulation. Large areas of spatial overlap were seen between F and M NBR (Fig. 3), thus answering the first aim of the study, in: contralateral regions surrounding the PBR, both superior and anterior to the site of the main activation; as well as throughout the ipsilateral cortex representing the completely unstimulated right visual hemifield. The spatial extent of the NBR varied between stimuli due to the different locations of the PBRs. NBR covered the largest area during the F stimulus and reduced in extent during FM because of the additional PBR to the M stimuli. NBR to M stimuli, whilst of weaker amplitude, occurred over as wide a range of visual regions as F stimuli, although the coverage of the M NBR was not as consistent or contiguous (Fig. 3). Our paradigm induced NBR in all retinotopic locations relative to the PBR, including inferior, superior peripheral, and foveal representations. This observation agrees with (Bressler et al., 2007; Pasley et al., 2007) and contrasts with (Wade and Rowland, 2010) whose peripheral bilateral visual ring did not induce foveal NBR for reasons that are unclear.

We further observe that the amplitude of the NBR varied between these regions and between the three stimulus conditions. This is interesting as it shows that the NBRs behaviour is more complex than simply appearing at the same amplitude in all unstimulated regions and suggests it isn't a blanket suppression, but is spatially specific. The regions showing the strongest magnitude NBR was similar between F and FM stimuli: posterior iV1 (Fig. 5E) and dorsal regions of visual cortex. Interestingly, although the dorsal visual NBR occurred bilaterally, it was considerably stronger in the contralateral hemisphere (Fig. 2). Therefore our data show two spatially distinct regions of peak NBR, in opposite hemispheres. Our ROI analysis shows further regional variation, in that the weakest NBR occurred in inferior visual regions (Fig. 5I&J). We also observed that F stimuli created much stronger NBR than M in superior peripheral regions (Fig. 5B). This is consistent with surround suppression effects (Muller and Kleinschmidt, 2004), as this ROI is furthest from the area of M PBR. Taken together these results show that the suppression of BOLD signal in visual cortex is highly dependent on the stimulus position.

5.2. *Modulation of NBR by stimulus characteristics*

Although we did not observe addition of F NBR and M NBR, we did observe that NBR amplitude increased substantially between M and F stimuli, the foveal stimulation showed a 50–200% larger magnitude NBR in superior cV1 and iV1 respectively. This shows that our task design did create modulation of responses and also that NBR amplitude was sensitive to stimulus characteristics, as previously reported for gabors

(Bressler et al., 2007). Although NBR was larger to F than to M stimuli, the NBR to M was not weak, showing amplitudes >0.6% in spatially opposite regions of posterior cV1 and iV1 and significantly above baseline levels in six out of the ten visual ROIs. Therefore we do not attribute the lack of NBR additivity to insufficient NBR in the M condition.

Modulation of NBR amplitude has been demonstrated by a number of previous studies whereby mean NBR magnitude increased with increasing stimulation intensity, both in visual and sensorimotor cortex (Klingner et al., 2010; Mayhew et al., 2016; Shmuel et al., 2002; Wilson et al., 2019) thereby enhancing both the afferent input and the strength of the NBR inducing signal. Mean DMN NBR magnitude has also been observed to increase with task difficulty (McKiernan et al., 2003; Singh and Fawcett, 2008). These scenarios differ from the current data in that in previous cases the receptive field size was unchanged between conditions, instead the frequency/amplitude of median nerve stimulation (Klingner et al., 2010), or frequency/duration of visual checkerboards (Shmuel et al., 2002) were increased. In the current study the F and M conditions stimulated distinct neural populations with different receptive fields. We suggest that these stimuli share an "NBR receptive field" in that they induce spatially overlapping visual NBR, but that this mechanism of triggering NBR does not lead to its modulation.

5.3. Spatial summation of BOLD responses

The spatial summation of BOLD responses has been sparsely investigated. An elegant study by Pasley et al. used bilateral ring stimuli to investigate how the amplitude of PBR was affected when it arose from different baseline states, a normal resting level and a lower baseline caused by a pre-existing NBR. They report that the amplitude of the PBR (as well as the cerebral blood flow and metabolic rate of oxygen consumption) was comparable between the two states, it reached the same peak value irrespective of the initial baseline level, suggesting the relative response amplitude depended on the baseline (Pasley et al., 2007). They did not investigate summation of NBRs however. Other work by Wade and Rowland compared peripheral BOLD responses during combinations of foveal and parafoveal bilateral grating rings at varying contrasts (Wade and Rowland, 2010). They found that NBR induced in peripheral visual cortex by a foveal stimulus was overridden by the addition of low contrast peripheral stimuli resulting in PBRs. These responses could be modelled as a multiplicative contrast gain control mechanism. Linear spatial summation of PBRs was observed in V1 to combinations of ring and wedge stimuli (Hansen et al., 2004). Kay et al., compared PBRs to partial-field visual stimuli that overlapped complementary portions of visual population receptive field (pRF) with PBRs to the sum of the stimuli (Kay et al., 2013). They reported sub additive effects across all visual cortex regions investigated (V1, V2, V3, LO) and for a range of visual stimulus types (noise patterns, checkers, gratings). They proposed a model of compressive spatial summation (CSS) to explain these results, which are supported by evidence of subadditivity in neural responses measured by electrocorticography in visual cortex (Winawer et al., 2013). Similarly, visual responses to simultaneous stimuli have been shown to be smaller than responses to the stimuli presented sequentially (Kastner et al., 2001). Our results extend this previous literature by specifically studying additivity of separate NBRs for the first time. By using two stimuli (F, M) that each separately induce NBR in visual regions we are able to study the effect on NBR of combining (FM) these two stimuli. We find no evidence of additivity between the two NBRs, the NBR to FM was sub-additive in being of smaller magnitude than the NBR summed (F + M) over separate stimuli, which is consistent with some previous reports of visual PBRs (Kay et al., 2013).

5.4. Possible pathways of NBR generation

The signalling pathways that may give rise to NBR remain obscure and difficult to study in detail with non-invasive imaging. Of particular interest is whether comparable mechanisms are responsible for generating different types of NBR, such as: contralateral NBR surrounding the PBR; and ipsilateral NBR in the opposite hemisphere. Although differing profoundly in location, these NBR share the common feature of occurring in unstimulated representations of the visual field, therefore reflecting a suppression of activity in areas not only unnecessary for completion of the current task but potentially sources of interfering or competing processing. We find no evidence of different response properties between NBR in iV1 and cV1, which we interpret as evidence that their generating mechanism was not modulated by our manipulation between separate and combined stimuli.

The local BOLD signal amplitude critically depends on the type of input to the region and the local balance of excitatory and inhibitory activity (Enager et al., 2009) as they determine the relative magnitudes of changes in cerebral blood flow (CBF) and cerebral metabolic rate of oxygen (CMRO2) (Buxton et al., 2014). But it remains unclear to what extent the neuronal and metabolic suppression underlying NBR results from a population level reduction in excitation, causing a net decrease in local metabolic demand, or activation of local inhibitory circuits (Iurilli et al., 2012; Lauritzen et al., 2012; Liepert et al., 2001; Pelled et al., 2009; Schafer et al., 2012; Smith et al., 2006; Sten et al., 2017). There exists a diverse range of distinct forms of cortical inhibitory neurons and their different functional properties are not well understood (Douglas and Martin, 2007), but the majority of them are GABAergic.

It has been demonstrated that interneurons can induce vasoconstriction as well as vasodilation (Cauli et al., 2004; Devor et al., 2007) and that positive allosteric modulators of $GABA_A$ receptors decrease CBF and BOLD signals (Matthew et al., 1995; Walter et al., 2016). However, the bulk of recent evidence suggests that activation of inhibitory neurons, resulting in a release of GABA, can lead to increases in cerebral blood flow (CBF) and BOLD signal (Anenberg et al., 2015; Enager et al., 2009; Lee et al., 2020; Pelled et al., 2009; Uhlirova et al., 2016; Vazquez et al., 2018), potentially via interaction with astrocytes and release of nitric oxide which is crucial to vasodilation (Iadecola, 2017; Vazquez et al., 2018).

We suggest that the most likely explanation of how increases in GABAergic activity can underlie NBR is via the synaptic and energetic efficiency of inhibitory neurons. Whereby due to their: small proportion (15–20%); low density of synaptic inputs (also ~20%), and lower energetic requirement for activation (Douglas and Martin, 2007; Duarte and Gruetter, 2013; Mangia et al., 2009; Patel et al., 2005), a small number of inhibitory cells can modulate the activity of a much larger population of excitatory cells with only a small energetic cost. Therefore the metabolic suppression caused by the reduced excitation out-weighs the increase in metabolism due to interneuron activity (Buzsáki et al., 2007; Mangia et al., 2009), which is supported by a recent 7T magnetic resonance spectroscopy study (Boillat et al., 2020). Or put another way, NBR arise as despite a small increase in energy use by inhibitory cells there is still a net energy saving due to the reduction in spiking in the majority of excitatory cells, leading to an overall decrease in CBF and $CMRO_2$ (Mullinger et al., 2014; Pasley et al., 2007).

In support of this, a recent optogenetic study in mice has shown that stimulation of somatostatin expressing (SST) interneurons can trigger a robust haemodynamic response which is surrounded by a negative response, mimicking an NBR (Lee et al., 2020). The surround NBR also showed a decrease in multi-unit spiking activity in deep cortical layers. This study provides the first clear suggestion that inhibitory neural activity can both increase local blood flow, suppress neural activity and decrease neighbouring haemodynamic signals. Although it could not conclude whether the ultimate cause of the suppression was SST interneurons projecting into the negative region, or suppressing excitatory input to that region (Lee et al., 2020).

Three primary mechanisms can be suggested to cause such an overall suppression of excitation: thalamocortical interaction (Logothetis et al., 2010); intra-cortical connectivity (Iurilli et al., 2012; Kastrup et al., 2008; Klingner et al., 2010, 2011) and top-down control of attention (Heinemann et al., 2009; Tootell et al., 1998) by fronto-parietal circuits

(Lauritzen et al., 2009). The contribution of these three mechanisms will depend on the brain region in question (e.g. intra modal, cross modal or DMN NBR) and exact experimental circumstances (e.g. type, intensity and amount of afferent sensory input, level of cognitive control required to complete task). A further complication for these interpretations is that thalamic input to the visual cortex can occur both through first order afference relaying retinal input via the LGN into cortical layer 4, or higher order via structures such as the pulvinar that relays information from the deep layers of one cortical area to the superficial layers of another region (Sherman, 2007).

The current experiment is unable to disambiguate them conclusively but we speculate that our data mostly indicate the action of an intra-cortical mechanism, whereby total stimulus drive is integrated into a single inhibitory input to the visual cortex NBR regions. A signal that doesn't summate over our combined stimulus inputs. Our favouring of a primarily cortical mechanism for the NBR we observe is supported by a lack of significant LGN activation during M stimulation (Fig. 2) despite that stimulus inducing widespread NBR in both visual hemispheres. This suggests that strong thalamic activity is not a prerequisite for cortical NBR.

Such intra-cortical influences would involve some initiation of NBR by the PBR region, involving lateral inhibition (Blakemore et al., 1970; Hopf et al., 2006; Muller and Kleinschmidt, 2004) effecting a surround suppression within the contralateral hemisphere as well as intra-hemispheric inhibitory effects via the white matter pathway passing through the splenium of the corpus callosum (Berlucchi, 2014) to act on iV1. How such local and distant mechanisms could result in similar NBR modulations should be investigated by future work, including the extent to which this process involves layer 6 pyramidal cells known to mediate widespread cortical inhibition by recruiting inhibitory neurons across the laminar (Bortone et al., 2014).

We expected little exertion of top-down control as our passive task had few attentional demands, making contributions from that third source minimal. We observed small PBR in dorsal intra-parietal sulcus regions responsible for spatial attention (Corbetta and Shulman, 2002) but no difference in this activity between conditions. We therefore cannot rule out the possible explanation that the FM NBR was not additive because the addition of the M to the F stimulus did not sufficiently increase the total attentional capture compared to F alone, and consequently did not induce additional NBR. Further work, possibly implementing effective connectivity and other promising modelling approaches (Havlicek et al., 2017) is necessary to further test the respective influences of these effects and to separate these mechanisms.

A key, but as yet unanswered question in understanding NBR is regards its exact functional purpose. The observed decreases in neuronal activity (Boorman et al., 2015; Shmuel et al., 2006) could arise: to minimise distracting input and reduce interfering communication from regions less-relevant to task execution forming a functional inhibition such as reported in electrophysiological literature (Jensen and Mazaheri, 2010; Mathewson et al., 2011); or as an energy saving mechanism whereby such regions are down-regulated to preserve metabolic efficiency (Buzsáki et al., 2007). In the former case, we expected that increased stimulation of one hemifield (e.g. FM vs F stimuli) would increase the requirement for suppression of the non-relevant hemifield. However, in this experiment there was perhaps not sufficient functional necessity for greater inhibition to be applied in the case of FM stimuli, if the passive task was not sufficiently demanding of cortical resources. A further possible complication in interpretation is whether the coherence of the checker reversal rate between the F and M stimuli resulted in a unified percept of the combined stimuli and that this resulted in nullifying any independent generation of NBR.

In conclusion we aimed to understand the contribution of checkerboard stimulation of foveal (F) and mid-eccentricity (M) locations of the left visual field to NBRs spatial occurrence and magnitude. The F and M stimuli had different retinotopic representations in visual cortex, resulting in non-overlapping PBRs, but overlapping NBRs throughout visual cortex, strongest in ipsilateral V1 and regions of contralateral V1 superior to the PBR. NBR were strongest to foveal (F) stimulation but also highly significant to a mid-eccentricity (M) stimulus.

The amplitude of the PBR did not increase at any location during combined FM stimuli, although the total spatial extent was largest to the FM stimulus. Despite this increase in the total amount of activated visual cortex the amplitude of the NBR was not different between the FM and the F stimuli, leading us to conclude that the addition of the M stimulus had no discernible effect on the NBR.

CRediT authorship contribution statement

Ross Wilson: Conceptualization, Formal analysis, Methodology, Visualization, Writing - original draft, Writing - review & editing. **Andrea Thomas:** Data curation, Formal analysis, Investigation. **Stephen D. Mayhew:** Conceptualization, Data curation, Formal analysis, Investigation, Methodology, Project administration, Software, Supervision, Validation, Visualization, Writing - original draft, Writing - review & editing.

Acknowledgements

The authors would like to thank Philips Healthcare Clinical Science for the provision of the multiband implementation and also to thank the CHBH, University of Birmingham for provision of scanner time.

Appendix A. Supplementary data

Supplementary data to this article can be found online at https://doi.org/10.1016/j.neuroimage.2020.116891.

References

Anenberg, E., Chan, A.W., Xie, Y., LeDue, J.M., Murphy, T.H., 2015. Optogenetic stimulation of GABA neurons can decrease local neuronal activity while increasing cortical blood flow. J. Cerebr. Blood Flow Metabol. 35, 1579–1586.
Berlucchi, G., 2014. Visual interhemispheric communication and callosal connections of the occipital lobes. Cortex 56, 1–13.
Bianciardi, M., Fukunaga, M., van Gelderen, P., de Zwart, J.A., Duyn, J.H., 2011. Negative BOLD-fMRI signals in large cerebral veins. J. Cerebr. Blood Flow Metabol. 31, 401–412.
Birn, R.M., Smith, M.A., Jones, T.B., Bandettini, P.A., 2008. The respiration response function: the temporal dynamics of fMRI signal fluctuations related to changes in respiration. Neuroimage 40, 644–654.
Blakemore, C., Carpenter, R.H., Georgeson, M.A., 1970. Lateral inhibition between orientation detectors in the human visual system. Nature 228, 37–39.
Boillat, Y., Xin, L., van der Zwaag, W., Gruetter, R., 2020. Metabolite concentration changes associated with positive and negative BOLD responses in the human visual cortex: a functional MRS study at 7 Tesla. J. Cerebr. Blood Flow Metabol. 40, 488–500.
Boorman, L., Harris, S., Bruyns-Haylett, M., Kennerley, A., Zheng, Y., Martin, C., Jones, M., Redgrave, P., Berwick, J., 2015. Long-latency reductions in gamma power predict hemodynamic changes that underlie the negative BOLD signal. J. Neurosci. 35, 4641–4656.
Boorman, L., Kennerley, A.J., Johnston, D., Jones, M., Zheng, Y., Redgrave, P., Berwick, J., 2010. Negative blood oxygen level dependence in the rat: a model for investigating the role of suppression in neurovascular coupling. J. Neurosci. 30, 4285–4294.
Bortone, D.S., Olsen, S.R., Scanziani, M., 2014. Translaminar inhibitory cells recruited by layer 6 corticothalamic neurons suppress visual cortex. Neuron 82, 474–485.
Bressler, D., Spotswood, N., Whitney, D., 2007. Negative BOLD fMRI response in the visual cortex carries precise stimulus-specific information. PloS One 2, e410.
Bressler, D.W., Fortenbaugh, F.C., Robertson, L.C., Silver, M.A., 2013. Visual spatial attention enhances the amplitude of positive and negative fMRI responses to visual stimulation in an eccentricity-dependent manner. Vision Res 85, 104–112.
Buxton, R.B., Griffeth, V.E., Simon, A.B., Moradi, F., 2014. Variability of the coupling of blood flow and oxygen metabolism responses in the brain: a problem for interpreting BOLD studies but potentially a new window on the underlying neural activity. Front. Neurosci. 8, 139.
Buzsáki, G., Kaila, K., Raichle, M., 2007. Inhibition and brain work. Neuron 56, 771–783.
Cauli, B., Tong, X.K., Rancillac, A., Serluca, N., Lambolez, B., Rossier, J., Hamel, E., 2004. Cortical GABA interneurons in neurovascular coupling: relays for subcortical vasoactive pathways. J. Neurosci. 24, 8940–8949.
Chang, C., Cunningham, J.P., Glover, G.H., 2009. Influence of heart rate on the BOLD signal: the cardiac response function. Neuroimage 44, 857–869.
Corbetta, M., Shulman, G.L., 2002. Control of goal-directed and stimulus-driven attention in the brain. Nat. Rev. Neurosci. 3, 201–215.

Devor, A., Tian, P., Nishimura, N., Teng, I.C., Hillman, E.M.C., Narayanan, S.N., Ulbert, I., Boas, D.A., Kleinfeld, D., Dale, A.M., 2007. Suppressed neuronal activity and concurrent arteriolar vasoconstriction may explain negative blood oxygenation level-dependent signal. J. Neurosci. 27, 4452–4459.
Devor, A., Ulbert, I., Dunn, A.K., Narayanan, S.N., Jones, S.R., Andermann, M.L., Boas, D.A., Dale, A.M., 2005. Coupling of the cortical hemodynamic response to cortical and thalamic neuronal activity. Proc. Natl. Acad. Sci. U. S. A. 102, 3822–3827.
Douglas, R.J., Martin, K.A., 2007. Recurrent neuronal circuits in the neocortex. Curr. Biol. 17, R496–R500.
Duarte, J.M., Gruetter, R., 2013. Glutamatergic and GABAergic energy metabolism measured in the rat brain by (13) C NMR spectroscopy at 14.1 T. J. Neurochem. 126, 579–590.
Enager, P., Piilgaard, H., Offenhauser, N., Kocharyan, A., Fernandes, P., Hamel, E., Lauritzen, M., 2009. Pathway-specific variations in neurovascular and neurometabolic coupling in rat primary somatosensory cortex. J. Cerebr. Blood Flow Metabol. 29, 976–986.
Feige, B., Scheffler, K., Esposito, F., Di Salle, F., Hennig, J., Seifritz, E., 2005. Cortical and subcortical correlates of electroencephalographic alpha rhythm modulation. J. Neurophysiol. 93, 2864–2872.
Ferbert, A., Priori, A., Rothwell, J.C., Day, B.L., Colebatch, J.G., Marsden, C.D., 1992. Interhemispheric inhibition of the human motor cortex. J Physiol 453, 525–546.
Fracasso, A., Luijten, P.R., Dumoulin, S.O., Petridou, N., 2018. Laminar imaging of positive and negative BOLD in human visual cortex at 7T. Neuroimage 164, 100–111.
Glover, G.H., Li, T.Q., Ress, D., 2000. Image-based method for retrospective correction of physiological motion effects in fMRI: RETROICOR. Magn. Reson. Med. 44, 162–167.
Gouws, A.D., Alvarez, I., Watson, D.M., Uesaki, M., Rodgers, J., Morland, A.B., 2014. On the role of suppression in spatial attention: evidence from negative BOLD in human subcortical and cortical structures. J. Neurosci. 34, 10347–10360.
Hairston, W.D., Hodges, D.A., Casanova, R., Hayasaka, S., Kraft, R., Maldjian, J.A., Burdette, J.H., 2008. Closing the mind's eye: deactivation of visual cortex related to auditory task difficulty. Neuroreport 19, 151–154.
Hansen, K.A., David, S.V., Gallant, J.L., 2004. Parametric reverse correlation reveals spatial linearity of retinotopic human V1 BOLD response. Neuroimage 23, 233–241.
Harel, N., Lee, S.-P., Nagaoka, T., Kim, D.-S., Kim, S.-G., 2002. Origin of negative blood oxygenation level-dependent fMRI signals. J. Cerebr. Blood Flow Metabol. 22, 908–917.
Havlicek, M., Ivanov, D., Roebroeck, A., Uludag, K., 2017. Determining excitatory and inhibitory neuronal activity from multimodal fMRI data using a generative hemodynamic model. Front. Neurosci. 11, 616.
Heeger, D.J., Huk, A.C., Geisler, W.S., Albrecht, D.G., 2000. Spikes versus BOLD: what does neuroimaging tell us about neuronal activity. Nat. Neurosci. 3, 631–633.
Heinemann, L., Kleinschmidt, A., Müller, N.G., 2009. Exploring BOLD changes during spatial attention in non-stimulated visual cortex. PloS One 4, e5560.
Hlushchuk, Y., Hari, R., 2006. Transient suppression of ipsilateral primary somatosensory cortex during tactile finger stimulation. J. Neurosci. 26, 5819–5824.
Hopf, J.M., Boehler, C.N., Luck, S.J., Tsotsos, J.K., Heinze, H.J., Schoenfeld, M.A., 2006. Direct neurophysiological evidence for spatial suppression surrounding the focus of attention in vision. Proc. Natl. Acad. Sci. U. S. A. 103, 1053–1058.
Huber, L., Goense, J., Kennerley, A.J., Ivanov, D., Krieger, S.N., Lepsien, J., Trampel, R., Turner, R., Moller, H.E., 2014. Investigation of the neurovascular coupling in positive and negative BOLD responses in human brain at 7 T. Neuroimage 97, 349–362.
Iadecola, C., 2017. The neurovascular unit coming of age: a journey through neurovascular coupling in health and disease. Neuron 96, 17–42.
Iurilli, G., Ghezzi, D., Olcese, U., Lassi, G., Nazzaro, C., Tonini, R., Tucci, V., Benfenati, F., Medini, P., 2012. Sound-driven synaptic inhibition in primary visual cortex. Neuron 73, 814–828.
Jenkinson, M., Bannister, P., Brady, M., Smith, S., 2002. Improved optimization for the robust and accurate linear registration and motion correction of brain images. Neuroimage 17, 825–841.
Jensen, O., Mazaheri, A., 2010. Shaping functional architecture by oscillatory alpha activity: gating by inhibition. Front. Hum. Neurosci. 4, 186.
Jerbi, K., Vidal, J.R., Ossandon, T., Dalal, S.S., Jung, J., Hoffmann, D., Minotti, L., Bertrand, O., Kahane, P., Lachaux, J.P., 2010. Exploring the electrophysiological correlates of the default-mode network with intracerebral EEG. Front. Syst. Neurosci. 4, 27.
Kannurpatti, S.S., Biswal, B.B., 2004. Negative functional response to sensory stimulation and its origins. J. Cerebr. Blood Flow Metabol. 24, 703–712.
Kasper, L., Bollmann, S., Diaconescu, A.O., Hutton, C., Heinzle, J., Iglesias, S., Hauser, T.U., Sebold, M., Manjaly, Z.M., Pruessmann, K.P., Stephan, K.E., 2017. The PhysIO toolbox for modeling physiological noise in fMRI data. J. Neurosci. Methods 276, 56–72.
Kastner, S., De Weerd, P., Pinsk, M.A., Elizondo, M.I., Desimone, R., Ungerleider, L.G., 2001. Modulation of sensory suppression: implications for receptive field sizes in the human visual cortex. J. Neurophysiol. 86, 1398–1411.
Kastrup, A., Baudewig, J., Schnaudigel, S., Huonker, R., Becker, L., Sohns, J.M., Dechent, P., Klingner, C., Witte, O.W., 2008. Behavioral correlates of negative BOLD signal changes in the primary somatosensory cortex. Neuroimage 41, 1364–1371.
Kay, K.N., Winawer, J., Mezer, A., Wandell, B.A., 2013. Compressive spatial summation in human visual cortex. J. Neurophysiol. 110, 481–494.
Klingner, C.M., Hasler, C., Brodoehl, S., Witte, O.W., 2010. Dependence of the negative BOLD response on somatosensory stimulus intensity. Neuroimage 53, 189–195.
Klingner, C.M., Huonker, R., Flemming, S., Hasler, C., Brodoehl, S., Preul, C., Burmeister, H., Kastrup, A., Witte, O.W., 2011. Functional deactivations: multiple ipsilateral brain areas engaged in the processing of somatosensory information. Hum. Brain Mapp. 32, 127–140.
Kwong, K.K., Belliveau, J.W., Chesler, D.A., Goldberg, I.E., Weisskoff, R.M., Poncelet, B.P., Kennedy, D.N., Hoppel, B.E., Cohen, M.S., Turner, R., 1992. Dynamic magnetic resonance imaging of human brain activity during primary sensory stimulation. Proc. Natl. Acad. Sci. U. S. A. 89, 5675–5679.
Lauritzen, M., Mathiesen, C., Schaefer, K., Thomsen, K.J., 2012. Neuronal inhibition and excitation, and the dichotomic control of brain hemodynamic and oxygen responses. Neuroimage 62, 1040–1050.
Lauritzen, T.Z., D'Esposito, M., Heeger, D.J., Silver, M.A., 2009. Top-down flow of visual spatial attention signals from parietal to occipital cortex. J. Vis. 9, 18 11–14.
Lee, L., Boorman, L., Glendenning, E., Christmas, C., Sharp, P., Redgrave, P., Shabir, O., Bracci, E., Berwick, J., Howarth, C., 2020. Key aspects of neurovascular control mediated by specific populations of inhibitory cortical interneurons. Cerebr. Cortex 30, 2452–2464.
Liepert, J., Dettmers, C., Terborg, C., Weiller, C., 2001. Inhibition of ipsilateral motor cortex during phasic generation of low force. Clin. Neurophysiol. 112, 114–121.
Logothetis, N.K., 2002. The neural basis of the blood-oxygen-level-dependent functional magnetic resonance imaging signal. Philos. Trans. R. Soc. Lond. B Biol. Sci. 357, 1003–1037.
Logothetis, N.K., Augath, M., Murayama, Y., Rauch, A., Sultan, F., Goense, J., Oeltermann, A., Merkle, H., 2010. The effects of electrical microstimulation on cortical signal propagation. Nat. Neurosci. 13, 1283–1291.
Logothetis, N.K., Pauls, J., Augath, M., Trinath, T., Oeltermann, A., 2001. Neurophysiological investigation of the basis of the fMRI signal. Nature 412, 150–157.
Mangia, S., Giove, F., Tkác, I., Logothetis, N.K., Henry, P.-G., Olman, C.A., Maraviglia, B., Di Salle, F., Uğurbil, K., 2009. Metabolic and hemodynamic events after changes in neuronal activity: current hypotheses, theoretical predictions and in vivo NMR experimental findings. J. Cerebr. Blood Flow Metabol. 29, 441–463.
Mathewson, K.E., Lleras, A., Beck, D.M., Fabiani, M., Ro, T., Gratton, G., 2011. Pulsed out of awareness: EEG alpha oscillations represent a pulsed-inhibition of ongoing cortical processing. Front. Psychol. 2.
Matthew, E., Andreason, P., Pettigrew, K., Carson, R.E., Herscovitch, P., Cohen, R., King, C., Johanson, C.E., Greenblatt, D.J., Paul, S.M., 1995. Benzodiazepine receptors mediate regional blood flow changes in the living human brain. Proc. Natl. Acad. Sci. U. S. A. 92, 2775–2779.
Mayhew, S.D., Hylands-White, N., Porcaro, C., Derbyshire, S.W., Bagshaw, A.P., 2013a. Intrinsic variability in the human response to pain is assembled from multiple, dynamic brain processes. Neuroimage 75, 68–78.
Mayhew, S.D., Mullinger, K.J., Ostwald, D., Porcaro, C., Bowtell, R., Bagshaw, A.P., Francis, S.T., 2016. Global signal modulation of single-trial fMRI response variability: effect on positive vs negative BOLD response relationship. Neuroimage 133, 62–74.
Mayhew, S.D., Ostwald, D., Porcaro, C., Bagshaw, A.P., 2013b. Spontaneous EEG alpha oscillation interacts with positive and negative BOLD responses in the visual-auditory cortices and default-mode network. Neuroimage 76, 362–372.
McKiernan, K.A., Kaufman, J.N., Kucera-Thompson, J., Binder, J.R., 2003. A parametric manipulation of factors affecting task-induced deactivation in functional neuroimaging. J. Cognit. Neurosci. 15, 394–408.
Mozolic, J.L., Joyner, D., Hugenschmidt, C.E., Peiffer, A.M., Kraft, R.A., Maldjian, J.A., Laurienti, P.J., 2008. Cross-modal deactivations during modality-specific selective attention. BMC Neurol. 8, 35.
Muller, N.G., Kleinschmidt, A., 2004. The attentional 'spotlight's' penumbra: center-surround modulation in striate cortex. Neuroreport 15, 977–980.
Mullinger, K.J., Mayhew, S.D., Bagshaw, A.P., Bowtell, R., Francis, S.T., 2014. Evidence that the negative BOLD response is neuronal in origin: a simultaneous EEG-BOLD-CBF study in humans. Neuroimage 94, 263–274.
Newton, J.M., Sunderland, A., Gowland, P.A., 2005. fMRI signal decreases in ipsilateral primary motor cortex during unilateral hand movements are related to duration and side of movement. Neuroimage 24, 1080–1087.
Ogawa, S., Lee, T.M., Kay, A.R., Tank, D.W., 1990. Brain magnetic resonance imaging with contrast dependent on blood oxygenation. Proc. Natl. Acad. Sci. U. S. A. 87, 9868–9872.
Pasley, B.N., Inglis, B.A., Freeman, R.D., 2007. Analysis of oxygen metabolism implies a neural origin for the negative BOLD response in human visual cortex. Neuroimage 36, 269–276.
Patel, A.B., de Graaf, R.A., Mason, G.F., Rothman, D.L., Shulman, R.G., Behar, K.L., 2005. The contribution of GABA to glutamate/glutamine cycling and energy metabolism in the rat cortex in vivo. Proc. Natl. Acad. Sci. U. S. A. 102, 5588–5593.
Pelled, G., Bergstrom, D.A., Tierney, P.L., Conroy, R.S., Chuang, K.H., Yu, D., Leopold, D.A., Walters, J.R., Koretsky, A.P., 2009. Ipsilateral cortical fMRI responses after peripheral nerve damage in rats reflect increased interneuron activity. Proc. Natl. Acad. Sci. U. S. A. 106, 14114–14119.
Puckett, A.M., Mathis, J.R., DeYoe, E.A., 2014. An investigation of positive and inverted hemodynamic response functions across multiple visual areas. Hum. Brain Mapp. 35, 5550–5564.
Raichle, M.E., MacLeod, A.M., Snyder, A.Z., Powers, W.J., Gusnard, D.A., Shulman, G.L., 2001. A default mode of brain function. Proc. Natl. Acad. Sci. U. S. A. 98, 676–682.
Raichle, M.E., Snyder, A.Z., 2007. A default mode of brain function: a brief history of an evolving idea. Neuroimage 37, 1083–1090 discussion 1097-1089.
Schafer, K., Blankenburg, F., Kupers, R., Gruner, J.M., Law, I., Lauritzen, M., Larsson, H.B., 2012. Negative BOLD signal changes in ipsilateral primary somatosensory cortex are associated with perfusion decreases and behavioral evidence for functional inhibition. Neuroimage 59, 3119–3127.
Sherman, S.M., 2007. The thalamus is more than just a relay. Curr. Opin. Neurobiol. 17, 417–422.

Shmuel, A., Augath, M., Oeltermann, A., Logothetis, N.K., 2006. Negative functional MRI response correlates with decreases in neuronal activity in monkey visual area V1. Nat. Neurosci. 9, 569–577.
Shmuel, A., Yacoub, E., Pfeuffer, J., Van de Moortele, P.F., Adriany, G., Hu, X., Ugurbil, K., 2002. Sustained negative BOLD, blood flow and oxygen consumption response and its coupling to the positive response in the human brain. Neuron 36, 1195–1210.
Singh, K.D., Fawcett, I.P., 2008. Transient and linearly graded deactivation of the human default-mode network by a visual detection task. Neuroimage 41, 100–112.
Smith, A.T., Cotillon-Williams, N.M., Williams, A.L., 2006. Attentional modulation in the human visual cortex: the time-course of the BOLD response and its implications. Neuroimage 29, 328–334.
Smith, A.T., Singh, K.D., Greenlee, M.W., 2000. Attentional suppression of activity in the human visual cortex. Neuroreport 11, 271–277.
Smith, A.T., Williams, A.L., Singh, K.D., 2004. Negative BOLD in the visual cortex: evidence against blood stealing. Hum. Brain Mapp. 21, 213–220.
Sten, S., Lundengard, K., Witt, S.T., Cedersund, G., Elinder, F., Engstrom, M., 2017. Neural inhibition can explain negative BOLD responses: a mechanistic modelling and fMRI study. Neuroimage 158, 219–231.
Tootell, R.B., Hadjikhani, N., Hall, E.K., Marrett, S., Vanduffel, W., Vaughan, J.T., Dale, A.M., 1998. The retinotopy of visual spatial attention. Neuron 21, 1409–1422.
Uhlirova, H., Kilic, K., Tian, P., Thunemann, M., Desjardins, M., Saisan, P.A., Sakadzic, S., Ness, T.V., Mateo, C., Cheng, Q., Weldy, K.L., Razoux, F., Vandenberghe, M., Cremonesi, J.A., Ferri, C.G., Nizar, K., Sridhar, V.B., Steed, T.C., Abashin, M., Fainman, Y., Masliah, E., Djurovic, S., Andreassen, O.A., Silva, G.A., Boas, D.A., Kleinfeld, D., Buxton, R.B., Einevoll, G.T., Dale, A.M., Devor, A., 2016. Cell type specificity of neurovascular coupling in cerebral cortex. Elife 5.
Vazquez, A.L., Fukuda, M., Kim, S.G., 2018. Inhibitory neuron activity contributions to hemodynamic responses and metabolic load examined using an inhibitory optogenetic mouse model. Cerebr. Cortex 28, 4105–4119.
Viswanathan, A., Freeman, R.D., 2007. Neurometabolic coupling in cerebral cortex reflects synaptic more than spiking activity. Nat. Neurosci. 10, 1308–1312.
Wade, A.R., Rowland, J., 2010. Early suppressive mechanisms and the negative blood oxygenation level-dependent response in human visual cortex. J. Neurosci. 30, 5008–5019.
Walter, S.A., Forsgren, M., Lundengard, K., Simon, R., Torkildsen Nilsson, M., Soderfeldt, B., Lundberg, P., Engstrom, M., 2016. Positive allosteric modulator of GABA lowers BOLD responses in the cingulate cortex. PloS One 11, e0148737.
Wandell, B.A., Dumoulin, S.O., Brewer, A.A., 2007. Visual field maps in human cortex. Neuron 56, 366–383.
Wilson, R., Mullinger, K.J., Francis, S.T., Mayhew, S.D., 2019. The relationship between negative BOLD responses and ERS and ERD of alpha/beta oscillations in visual and motor cortex. Neuroimage 199, 635–650.
Winawer, J., Kay, K.N., Foster, B.L., Rauschecker, A.M., Parvizi, J., Wandell, B.A., 2013. Asynchronous broadband signals are the principal source of the BOLD response in human visual cortex. Curr. Biol. 23, 1145–1153.